RESEARCH NOTE

Open Access

Measuring and visualizing scattered x-rays using red–green–blue (RGB) heat maps during extracorporeal membrane oxygenation in the intensive care unit

Tomihiko Daioku[1*], Fumiko Oishi[2], Masanao Kobayashi[3], Naoko Arakawa[1] and Harumi Ejiri[1]

Abstract

Objective This study investigated the continuous risks of scattered radiation associated with a series of procedures—from extracorporeal membrane oxygenation (ECMO) cannulation through to enteral feeding tube insertion—in an intensive care unit (ICU) setting by visualizing the dose distribution using a red–green–blue (RGB) color map.

Results The scattered radiation doses were measured at 80 points around a tissue-equivalent phantom using calibrated nanoDot dosimeters, and an RGB color map was generated to visualize the dose intensity. Radiation doses near the X-ray source reached 783.6 μSv/hour at 50 cm, exceeding annual public exposure limits within 1 h. These findings emphasize the importance of using appropriate radiation protection equipment, suggesting that distance is a key factor in reducing the ICU exposure risk. They also offer practical guidance for planners involved in radiation safety management in hospital settings.

Keywords Extracorporeal membrane oxygenation, Intensive care unit, Red–green–blue, Scattered X-rays

Introduction

Extracorporeal membrane oxygenation (ECMO) is effective in patients with severe pneumonia, including those with coronavirus disease 2019 (COVID-19) [1–4]. Veno-venous (V-V) ECMO can be easily cannulated percutaneously and is widely used in emergency situations. Percutaneous cannulation of V-V ECMO can be achieved with a high success rate and low complication rate under ultrasound and fluoroscopic guidance [5]. However, because X-rays are used for fluoroscopic guidance, the medical staff involved in treatment cannot avoid radiation exposure.

Scattered radiation occurs when the primary beam of X-rays scatters during irradiation, and the surrounding medical personnel are often exposed to this scattered radiation [6]. In radiography, occupational exposure caused by scattered radiation from a single examination is negligible; however, in fluoroscopy, long-term exposure to such scattered radiation increases the risk of cancer, cataracts, and skin damage [7–9].

In the intensive care unit (ICU), procedures such as ECMO cannulation and subsequent enteral feeding tube insertion typically involve emergency physicians or

*Correspondence:
Tomihiko Daioku
t-daioku@fsc.chubu.ac.jp
[1]Department of Nursing, College of Life and Health Sciences, Chubu University, Kasugai, Japan
[2]School of Health Sciences, Faculty of Radiological Technology, Fujita Health University, Toyoake, Japan
[3]School of Nursing, Seirei Christopher Introduction University, Hamamatsu, Japan

intensivists, nurses, and clinical engineers. Physicians performing cannulation are positioned closest to the patient, who acts as the radiation source, and therefore are expected to receive the highest radiation exposure. Similarly, nurses assisting the procedure are also positioned relatively close to the radiation source and are at increased risk of radiation exposure. Therefore, they are generally required to wear appropriate radiation protection equipment during such procedures. In contrast, clinical engineers are primarily responsible for priming and managing the ECMO device and typically work at a greater distance from the radiation source. Consequently, they are considered to be at lower risk of exposure and may not always wear radiation protection gear, although this practice should be carefully evaluated in light of safety standards.

Emergency physicians, intensive care physicians, nurses, and clinical engineers are experts in patient management and do not necessarily have specialized knowledge of radiation. Non-radiation medical professionals have little knowledge of radiation safety and insufficient awareness of risk perception [10–12], and even if they underwent training, it does not directly translate into improved behavior [13, 14]. Providing an environment wherein medical professionals without specialized knowledge of radiation can easily imagine the risk of exposure and safely concentrate on the medical procedure at hand is necessary.

Previous studies have shown radiation levels using contour maps or numbers, making it difficult for medical professionals without specialized knowledge of radiation or radiation exposure to intuitively understand risks [15–17]. In recent years, Monte Carlo simulations have been used to provide a 4D distribution of scattered radiation to medical professionals without radiation expertise, demonstrating the effectiveness of visual information [18, 19]. Virtual reality experiences have been proposed as a tool for visually grasping radiation threats, but doubts have been raised about their versatility, particularly due to the complexity of equipment setup and concerns over cost-effectiveness, and they have not yet been widely put into practical use [20].

This study measured scattered radiation during ECMO cannulation in the ICU and developed a versatile visual tool for enhancing radiation safety awareness among healthcare providers.

Main text

Methods

We measured the amount of scattered radiation generated during cannulation and subsequent enteral feeding tube insertion under fluoroscopic guidance while initiating ECMO in the ICU. The data obtained were displayed on a color map.

Period and measurement location

Measurements were conducted in the Fujita Health University Hospital ICU in Japan in September 2021. Care was taken not to interfere with the regular medical treatment during the experiment.

Equipment and methods used

The X-ray generator used was OEC 9900 Elite (GE Healthcare, Chicago, IL, USA). A RAN110 RANDO anthropomorphic phantom (height: 175 cm, weight: 70 kg; The Phantom Laboratory, Salem, MA, USA) was used as the human equivalent. Scattered radiation was measured using a nanoDot dosimeter (Nagase Landauer Co., Ltd., Ibaraki, Japan). Dose profiles and color maps were created using OriginPro 2019s (Lightstone Co., Ltd., Tokyo, Japan).

Irradiation conditions

The irradiation conditions were set based on the advice of three radiologists with 3–15 years of experience in this procedure: tube voltage, 80 kVp; tube current, 3.2 mA; pulse rate, 8 f/s; and exposure time, 20 min. Under these conditions, the Rand phantom was irradiated with X-rays, and the amount of scattered radiation generated was measured using nanodots. Under the specified irradiation conditions, the nanoDot dosimeter (Nagase Landauer) positioned the farthest from the irradiation field exhibited dose readings below the detection limit. Therefore, the irradiation duration was extended by a factor of five, resulting in a total exposure time of 100 min. The measured dose was subsequently normalized to a standard exposure time of 20 min for analysis. This approach was used to minimize the measurement errors.

Measurement

For the measurement of scattered radiation, the jungle gym method using a paper tube and plastic joint with an inner diameter of 2.5 cm, thickness of 0.3 cm, density of 0.75 g/cm^3, and length of 50 cm was adopted [21]. For the measurements of dose, the nanoDot optically stimulated luminescence dosimeters (OSL dosimeters) (Fig. 1). The measurement points were located 100 cm above the floor, corresponding to the coronal plane of the Landau phantom, and spaced 50 cm from the centerline (Fig. 2).

Each nanoDot dosimeter was calibrated, and the readings were converted to air kerma values for analysis. The nanoDot dosimeter was placed with individual element faces facing the central ray to minimize the direction dependence [22]. Calibration constants of the nanoDot dosimeter were obtained by alternating irradiation under the same conditions, with the element placed on the surface of water, equivalent to the plate phantom, and ionization chamber dosimeter (model 9015; Radcal, Monrovia, CA, USA) in free air. The radiation dose

Fig. 1 Image of X-ray device, phantom, and nanodot arrangement

measured using the nanoDot dosimeter represents the ambient dose. In this study, to estimate the personal dose equivalent at a depth of 1 cm, Hp(10), as an indicator of radiation exposure to the human body, the raw readings from the nanoDot dosimeter were corrected by applying a calibration factor and a backscatter correction coefficient of 1.4, according to the following formula:

Hp(10) = nanoDot reading × calibration factor × backscatter correction coefficient (1.4).

Heat map generation

The measurement data were represented as a red–green–blue (RGB) color map generated using OriginPro 2019 (Lightstone Co., Ltd.).

A two-dimensional heat map was generated based on the measurements obtained at 80 points (Fig. 2). To estimate the values between the measured points, interpolation was performed using the inverse square law of the distance from the center point. Herein, the "two-dimensional vector from the center point" refers to a mathematical representation of each measurement point's spatial relationship relative to the central reference point. This vector is defined by the coordinates of the measurement and center points, where the distance between them is calculated using the Euclidean norm.

For interpolation, the inverse square law of distance was applied to adjust the weight of each measurement point in proportion to its distance from the center. Specifically, the interpolated value I at a given grid location was calculated using the formula:

$$I = \frac{\sum_{i=1}^{n}\left(\frac{M_i}{d_i^2}\right)}{\sum_{i=1}^{n}\left(\frac{1}{d_i^2}\right)}$$

where Mi is the measured value at point i, di is the Euclidean distance from the center to point i, and n is the total number of measured points. This formulation ensures that nearby measurements exert a stronger influence than distant ones per the inverse-square principle.

This approach ensures that data points closer to the center contribute more heavily to the interpolation process, whereas data points farther away have diminished influence. By applying this weighting scheme, the method produces a more accurate and spatially consistent heat map that reflects variations in the measurements with smoother transitions.

Following this interpolation step, spline interpolation was applied to smooth the resulting data. Spline interpolation was performed in two dimensions using a bicubic spline method, which minimizes curvature across both axes and ensures continuity in the first and second derivatives. Spline interpolation fits a smooth curve through points to remove any abrupt changes and enhances the visual continuity of the heat map, leading to a high-quality and visually consistent representation of the spatial data distribution. Finally, the heat map was output at a resolution of 150 dpi to ensure high graphical fidelity, providing an effective means of visualizing the spatial relationships and gradients within the dataset.

Results

Table 1 presents the measured values of scattered radiation generated during fluoroscopic procedures for ECMO cannulation and subsequent insertion of an enteral feeding tube."

The dose distribution of scattered radiation generated by fluoroscopy during cannulation of an ECMO in the ICU was visualized in an RGB format (Fig. 3). This initiative will allow medical professionals to visually assess the amount of radiation that they may receive during treatment.

Scattered radiation was widely distributed in the patient's left and right directions. However, little spread was observed on the patient's head or tail. Typically, during ECMO cannulation and the subsequent enteral feeding tube insertion procedure, the surgeon is positioned to the right of the patient, and the first caregiver is positioned to the right of the surgeon (Fig. 2). The RGB dose map shows that the areas where the surgeon and caregiver perform the procedure are exposed to the highest radiation dose owing to scattered radiation. The dose map shows that the first caregiver received a higher radiation dose than the surgeon.

The highest radiation dose from the scattered radiation was within 100 cm to the right of the patient. However, at a distance of 200 cm from the radiation field, the radiation dose was < 100 μSv/hour. Our findings highlight

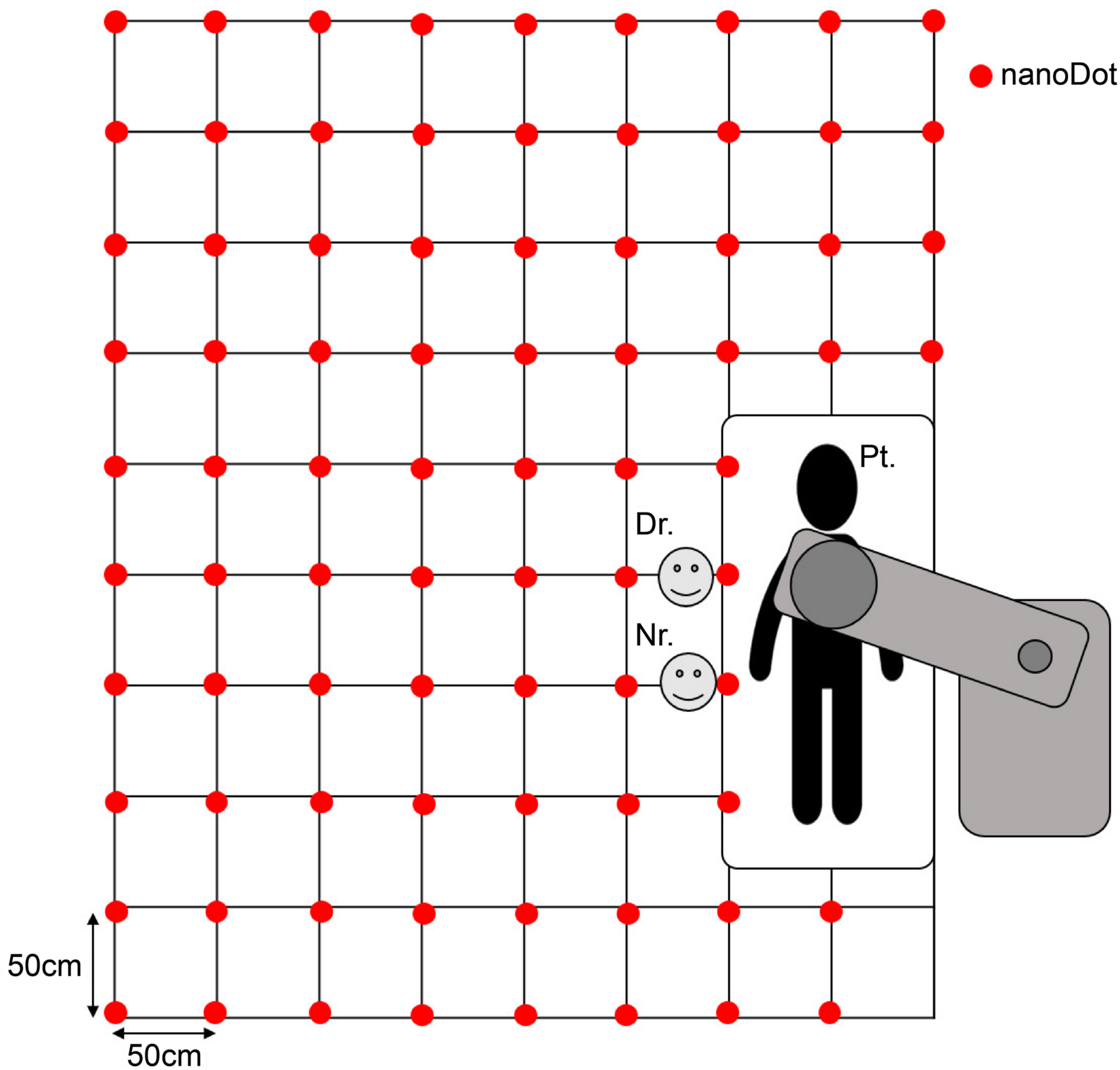

Fig. 2 Measurement points. Dr. indicates the area where the surgeon usually works, whereas Ns. indicates the area where the first caregiver usually works

the importance of distance and location in radiation protection.

Discussion

Scattered radiation, the primary cause of occupational radiation exposure, is generated by objects in the path of a primary X-ray beam, with the patient being the main source. Although the radiation dose received by medical staff during a single examination is lower than that received by patients, the cumulative lifetime dose can be significant because medical staff perform similar examinations and treatments daily. The radiation dose from the scattered radiation generated by X-ray fluoroscopy during ECMO cannulation and enteral feeding tube insertion into the ICU was visualized using an RGB color map. This initiative will enable ICU staff to easily recognize the risks of radiation exposure even if they do not have specialized knowledge of radiation. Tools for visualizing scattered radiation distribution and intensity can also be used as part of radiation protection education, helping healthcare professionals optimize their positioning and minimize radiation exposure [7].

Radiation protection for operators

Healthcare professionals involved in radiation-related tasks may be exposed to low-dose radiation over

Table 1 Personal dose equivalent, Hp(10), at each measurement point

Distance from the source		Personal dose equivalent (Hp 10)	Distance from the source		Personal dose equivalent (Hp 10)
X [cm]	Y [cm]	µSv/hr	X [cm]	Y [cm]	µSv/hr
-350	250	2.54	-150	0	79.82
-350	200	6.78	-150	-50	70.56
-350	150	4.80	-150	-100	51.55
-350	100	6.29	-150	-150	37.11
-350	50	7.52	-150	-200	25.22
-350	0	4.87	-100	250	18.55
-350	-50	6.43	-100	200	20.96
-350	-100	5.91	-100	150	41.44
-350	-150	4.19	-100	100	51.74
-350	-200	2.69	-100	50	114.50
-300	250	10.43	-100	0	199.60
-300	200	26.90	-100	-50	193.86
-300	150	19.78	-100	-100	121.31
-300	100	25.25	-100	-150	70.28
-300	50	30.03	-100	-200	31.40
-300	0	18.50	-50	250	37.80
-300	-50	26.52	-50	200	47.40
-300	-100	23.95	-50	150	42.60
-300	-150	16.89	-50	100	69.00
-300	-200	10.80	-50	50	248.14
-250	250	4.61	-50	0	783.90
-250	200	10.29	-50	-50	676.97
-250	150	18.55	-50	-100	220.73
-250	100	26.58	-50	-150	72.96
-250	50	28.73	-50	-200	21.39
-250	0	42.90	0	250	19.80
-250	-50	27.83	0	200	31.80
-250	-100	33.58	0	150	38.40
-250	-150	40.51	0	100	64.20
-250	-200	26.84	0	50	ND
-200	250	20.29	0	0	ND
-200	200	6.15	0	-50	ND
-200	150	27.93	0	-100	ND
-200	100	40.13	0	-150	73.20
-200	50	39.89	0	-200	21.60
-200	0	47.64	50	250	25.80
-200	-50	48.25	50	200	41.40
-200	-100	32.47	50	150	31.80
-200	-150	35.20	50	100	84.60
-200	-200	25.89	50	50	248.40
-150	250	18.87	50	0	783.90
-150	200	19.76	50	-50	676.97
-150	150	22.17	50	-100	220.73
-150	100	40.58	50	-150	72.96
-150	50	51.66	50	-200	21.39

extended periods. Prolonged exposure to low-dose radiation has been associated with an increased risk of cataracts and elevated cancer risk in healthcare workers [23, 24].

Medical personnel directly involved in this procedure are forced to work within 50–100 cm of the center of the incident X-ray. Healthcare workers in this location, especially surgeons and nurses, may reach the general public exposure limit in approximately 1 h and exceed the

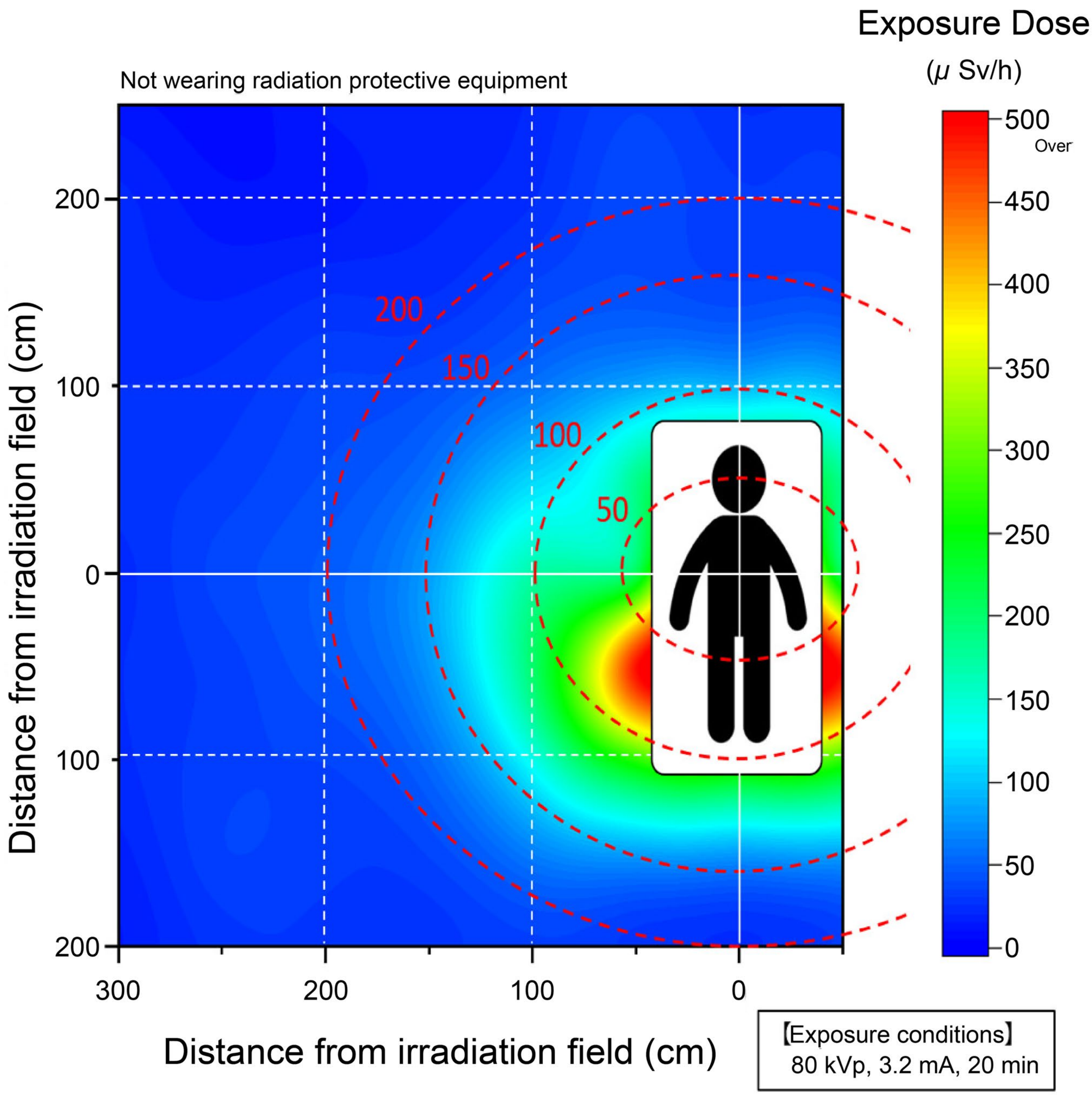

Fig. 3 RGB visual of scattered X-rays when introduced into ECMO in the ICU. In the RGB dose map, areas with high exposure are represented in red, areas with medium exposure in green, and areas with low exposure in blue

occupational exposure limit if they perform treatment twice a month. The distribution intensity of the scattered radiation was stronger on the patient's foot side. If the first caregiver had provided care from the left side of the surgeon, the radiation exposure dose on the right side of the patient's face would have been 248.14 μSv/hour, which could have reduced radiation exposure by up to approximately 70%.

Although reducing the radiation exposure to the left side of the surgeon, that is, the right side of the patient's face, is possible, there is still sufficient radiation exposure to cause health damage. Therefore, we recommend that medical professionals who directly treat patients use appropriate radiation protection equipment, such as radiation protection aprons and protective glasses. The use of radiation protection equipment (especially lead aprons) provides very high radiation shielding effects; depending on the thickness and material of the apron used, lead aprons have an average shielding efficiency of 80–95% against 60–120 kV X-rays [25]. However, even if radiation protection equipment is used properly, a risk of non-uniform exposure remains. To reduce radiation exposure, completing the cannulation procedure as quickly as possible is important.

Radiation protection for non-operators

The scattered radiation spread strongly to the left and right from the center of the incident X-ray, slightly toward the patient's feet, with a radius of approximately 150 cm. Beyond a radius of 200 cm, the radiation dose was almost equal to the background radiation dose. The radiation doses at distances of 100 and 200 cm from the center of the incident X-rays were significantly different, highlighting the importance of distance.

Many medical staff members are involved in the ECMO cannulation. Staff should not be involved in direct cannulation procedures but wait in the examination room for priming equipment or managing respiratory and circulatory care work at least 200 cm away from the patient. The dose received by staff who were > 200 cm away from the patient was only 1/1000th of the dose that can cause cancer [26], and it is highly unlikely that the aforementioned dose limit will be exceeded. As scattered radiation tends to be widely distributed on both sides of the patient, working on the head or foot side, if possible, will reduce the risk of exposure.

Impact and expectations of environmental factors

Data collection was conducted in a standard-sized single-occupancy ICU room in Japan. In cases involving patients requiring ECMO, various medical devices such as ventilators and multiple infusion or injection pumps are typically used, and these devices may partially attenuate scattered radiation. However, such clinical setups vary depending on individual patients, and it is of limited significance to replicate them precisely in a simulation. Rather, in situations where recreating specific setups is challenging, it is important to simulate under the assumption of a worst-case scenario [27]. In this case, since surrounding medical equipment and radiation protective devices may attenuate but are unlikely to amplify scattered radiation, it was considered meaningful to perform measurements in an environment with minimal shielding whenever possible. Therefore, the map generated in this study enables healthcare professionals involved in this procedure to work more safely without underestimating their own radiation exposure risk.

Other visual tools, such as virtual reality, are suitable for routine training as they provide a more realistic experience; however, they are not ideal for risk management briefings immediately before a procedure due to the time required for equipment setup. While the map generated in this study may appear simple at first glance, it is highly valuable for the final checks before task initiation. Therefore, it is believed that such hazard maps can be applied in ICUs and various radiation departments, including X-ray and CT examination rooms.

Limitations

This study had a limitation. The results of the dose map showed that the radiation dose received by the staff assisting the surgeon next to them may be higher than that received by the surgeon. In general, the cathode side of the C-arm has higher X-ray output; in this case, the cathode was located on the patient's right leg [28]. This phenomenon varies depending on the equipment type used and the insertion angle of the C-arm. However, distance is an important factor in scattered radiation exposure during examinations, and the dose is particularly high within 100 cm of the patient. Therefore, collecting more detailed data on scattered radiation intensity, especially near the patient, using equipment used in clinical settings, and analyzing trends are necessary. By clarifying trends of scattered radiation distribution intensity, appropriate locations for providing treatment and assistance from the perspective of radiation protection can be determined.

In this study, anthropomorphic phantoms were used in place of actual human subjects, which introduces certain limitations. Specifically, phantoms cannot fully replicate the anatomical and physiological characteristics of the human body, such as variations in tissue composition, bone density, and fat distribution, all of which influence radiation attenuation and scattering. Furthermore, phantoms are inherently static and therefore, unable to simulate the dynamic elements present in real clinical settings, including patient respiration, movement, and procedural adjustments made by medical staff. These differences may limit the direct applicability of the findings to actual clinical environments.

While the present study simulates a single procedure within a spatially static environment, it lacks reproducibility in realistic dynamic settings involving factors such as patient respiration, body movements, and healthcare provider activity. In recent years, advanced computational techniques for modeling complex network structures—namely hyperbolic geometry and graph neural networks (GNNs)—have garnered increasing attention [29]. Although these methods are not yet widely adopted in the medical field, they hold great promise as tools for visualizing and predicting scattered radiation distribution during X-ray imaging and fluoroscopic procedures, particularly through the integration of hyperbolic representations, GNNs, and dynamic graph modeling.

Conclusions

In this study, the importance of distance for radiation protection was reaffirmed. Thus, operators must use appropriate radiation protection equipment. Radiation exposure significantly decreased when the distance was > 200 cm. In particular, the spread of scattered radiation to the head and feet of the patients was minimal. Therefore, non-operators could reduce radiation exposure by working 200 cm away from the patient and, if possible, on the head or foot side of the patient. The RGB dose map can be a useful tool for medical professionals to intuitively understand radiation exposure risk. This study's results provide evidence-based guidance for planners and practitioners involved in the management of radiation safety in healthcare environments.

Abbreviations

ECMO	Extracorporeal membrane oxygenation
ICU	Intensive care unit
COVID-19	Coronavirus disease 2019
RGB	Red–green–blue

Acknowledgements
Not applicable.

Author contributions
TD was responsible for the overall study conceptualization and study design, data collection, data analysis and interpretation, manuscript writing, and funding. FO contributed to conceptualization, study design, and data analysis and interpretation. MK contributed to data collection (setting the conditions for X-ray exposure), data analysis (reading radiation doses), and interpretation. NA contributed to the analysis (analysis of RGB heatmaps) and interpretation of the data. HE contributed to the supervision and project management. All authors read and approved the final manuscript.

Funding
This study was supported by JSPS KAKENHI (grant number: JP22K17462). The funder had no role in the conceptualization, design, data collection, analysis, decision to publish, or preparation of the manuscript,

Data availability
The datasets used and/or analysed during the current study are available from the corresponding author on reasonable request.

Declarations

Ethics approval and consent to participate
Since this study did not involve any human participants, human data, or human tissues (only a human-equivalent phantom was used), ethics approval, Declaration of Helsinki compliance, and consent to participate are not applicable and also deemed unnecessary as per the ethical guidelines of Chubu University based on Declaration of Helsinki.

Consent for publication
Not applicable.

Competing interests
The authors declare no competing interests.

Received: 16 March 2025 / Accepted: 6 May 2025
Published online: 16 May 2025

References

1. Bartlett RH, Ogino MT, Brodie D, McMullan DM, Lorusso R, MacLaren G, et al. Initial ELSO guidance document: ECMO for COVID-19 patients with severe cardiopulmonary failure. ASAIO J. 2020;66:472–4.
2. Munshi L, Walkey A, Goligher E, Pham T, Uleryk EM, Fan E. Venovenous extracorporeal membrane oxygenation for acute respiratory distress syndrome: a systematic review and meta-analysis. Lancet Respir Med. 2019;7:163–72.
3. Combes A, Hajage D, Capellier G, Demoule A, Lavoué S, Guervilly C, et al. Extracorporeal membrane oxygenation for severe acute respiratory distress syndrome. N Engl J Med. 2018;378:1965–75.
4. Peek GJ, Mugford M, Tiruvoipati R, Wilson A, Allen E, Thalanany MM, et al. Efficacy and economic assessment of conventional ventilatory support versus extracorporeal membrane oxygenation for severe adult respiratory failure (Cesar): a multicentre randomised controlled trial. Lancet. 2009;374:1351–63.
5. Burns J, Cooper E, Salt G, Gillon S, Camporota L, Daly K, et al. Retrospective observational review of percutaneous cannulation for extracorporeal membrane oxygenation. ASAIO J. 2016;62:325–8.
6. Jentzsch T, Pietsch CM, Stigler B, Ramseier LE, Seifert B, Werner CML. The compliance with and knowledge about radiation protection in operating room personnel: a cross-sectional study with a questionnaire. Arch Orthop Trauma Surg. 2015;135:1233–40.
7. Ylimaula S, Räsänen L, Hurskainen M, Peuna A, Julkunen P, Nieminen MT, et al. X-ray scatter in projection radiography. Radiat Prot Dosimetry. 2024;200:120–9.
8. Milacic S. Risk of occupational radiation-induced cataract in medical workers. Med Lav. 2009;100:178–86.
9. Mastrangelo G, Fedeli U, Fadda E, Giovanazzi A, Scoizzato L, Saia B. Increased cancer risk among surgeons in an orthopaedic hospital. Occup Med (Lond). 2005;55:498–500.
10. Alotaibi AE, Muhyi NA. Assessing the radiation protection knowledge among non-radiologists. IJMDC. 2019;3:159–62.
11. Indukuri S, Easwaramoorthy V. Awareness of radiation protection safety and hazards among healthcare workers and paramedical students. IJSR. 2021;10:491–515.
12. Masujima Y, Noto Y. Investigation about recognition of occupational exposure and radiation education in nurses engaged in intervention radiology. J Radiol Nurs. 2018;6:12–21. (in Japanese).
13. Algohani KA, Aldahhasi AA, Algarni AH. Awareness of radiation protection measures among radiologists and non-radiologists. Egypt J Hosp Med. 2018;70:371–5.
14. Kim TH, Hong SW, Woo NS, Kim HK, Kim JH. The radiation safety education and the pain physicians' efforts to reduce radiation exposure. Korean J Pain. 2017;30:104–15.
15. Haqqani OP, Agarwal PK, Halin NM, Iafrati MD. Defining the radiation scatter cloud in the interventional suite. J Vasc Surg. 2013;58:1339–45.
16. Wagner M, Dresing K, Ludwig W, Ahrens CA, Bott OJ. SIScaR-GPU: fast simulation and visualization of intraoperative scattered radiation to support radiation protection training. Stud Health Technol Inf. 2012;180:968–72.
17. Giordano BD, Baumhauer JF, Morgan TL, Rechtine GR 2. Cervical spine imaging using mini–C-arm fluoroscopy: patient and surgeon exposure to direct and scatter radiation. J Spinal Disord Tech. 2009;22:399–403.
18. Fujibuchi T, Nakashima M, Arakawa H, Miyazaki H, Anam C. Evaluation of radiation protection effectivity in a cardiac angiography room using visualized scattered radiation distribution. J Radiol Prot. 2024;44.
19. Fujibuchi T. Radiation protection education using virtual reality for the visualisation of scattered distributions during radiological examinations. J Radiol Prot. 2021;41.
20. Daioku T, Kobayashi M, Oishi F. Development of visual educational materials for radiation protection in computed tomography. J Radiol Nurs. 2021;40:268–74.
21. Nakamura T, Shoichi S, Takei Y, Kobayashi M, Cruz V, Kobayashi I, et al. A more accurate and safer method for the measurement of scattered radiation in X-ray examination rooms. Radiol Phys Technol. 2020;13:69–75.
22. Okazaki T, Hayashi H, Takegami K, Okino H, Kimoto N, Maehata I, et al. Fundamental study of nanodot OSL dosimeters for entrance skin dose measurement in diagnostic X-ray examinations. J Radiat Prot Res. 2016;41:229–36.
23. Vano E, Kleiman NJ, Duran A, Rehani MM, Echeverri D, Cabrera M. Radiation cataract risk in interventional cardiology personnel. Radiat Res. 2010;174:490–5.
24. Wang JX, Zhang LA, Li BX, Zhao YC, Wang ZQ, Zhang JY, et al. Cancer incidence and risk Estimation among medical x-ray workers in China, 1950–1995. Health Phys. 2002;82:455–66.

25. Revathy P, Kaginelli SB. Quality assurance of lead aprons for radiation protection. Radiat Prot Dosimetry. 2023;199:2491–4.
26. Preston DL, Ron E, Tokuoka S, Funamoto S, Nishi N, Soda M, et al. Solid cancer incidence in atomic bomb survivors: 1958–1998. Radiat Res. 2007;168:1–64.
27. Casiraghi M, Albertini F, Lomax AJ. Advantages and limitations of the 'worst case scenario' approach in IMPT treatment planning. Phys Med Biol. 2013;58:1323–39.
28. Fung KK, Gilboy WB. Anode heel effect on patient dose in lumbar spine radiography. Br J Radiol. 2000;73:531–6.
29. Zhangyu M, Xiao B, Dianguo L, Wen X, Fan Y, Hao W. DHHNN. A dynamic hypergraph hyperbolic neural network based on variational autoencoder for multimodal data integration and node classification. Inf Fusion. 2025;119.

Publisher's note